

Matrix-Isolation and Ab Initio Study of the HKrCl⋯HCl Complex

Alice Corani, Alexandra Domanskaya, Leonid Khriachtchev,* Markku Räsänen, and Antti Lignell†

Laboratory of Physical Chemistry, P.O. Box 55, FIN-00014 University of Helsinki, Finland

Received: May 13, 2009; Revised Manuscript Received: August 21, 2009

The HKrCl complex with HCl is characterized by IR spectroscopy in a Kr matrix and by ab initio calculations. The HKrCl⋯HCl complex exhibits a strong blue shift of the H–Kr stretching mode in comparison with the HKrCl monomer, which indicates stabilization of the H–Kr bond upon complexation. The obtained maximal shift of ca. +300 cm⁻¹ is probably the largest blue shift experimentally observed for 1:1 molecular complexes. The HCl absorptions are found to be strongly red-shifted upon complexation with HKrCl (up to ca. -500 cm⁻¹). In the HKrCl synthesis procedure, an HCl/Kr matrix was first photolyzed at 193 nm to yield H and Cl atoms in a Kr matrix and then annealed at about 30 K to activate mobility of H atoms and to promote the H + Kr + Cl reaction. The HKrCl⋯HCl complex is mainly formed from the Cl⋯HCl intermediate complex that is produced by photolysis of HCl dimers. Bands of the HKrCl⋯(HCl)₂ complex are tentatively identified with a very large shift of ca. +700 cm⁻¹ for the H–Kr stretching mode. These experimental observations are supported and explained by ab initio calculations.

1. Introduction

The family of noble-gas hydrides HNgY is a part of modern noble-gas chemistry demonstrating fascinating properties (Ng = Ar, Kr, and Xe; Y is an electronegative fragment).^{1–4} A useful method to prepare these species includes photodissociation of HY precursors and thermal mobilization of H atoms in noble-gas matrices. The HNgY molecules are relatively weakly bound and show a strong (HNg)⁺Y⁻ charge-transfer character, which explains the observed large host effects reflected in extensive splitting and shifts of the absorption bands.¹

HKrCl is one of the noble-gas hydrides thoroughly studied in matrix-isolation experiments.^{5–9} This molecule is formed during 193 nm photolysis of HCl/Kr matrices, evidencing the locality of solid-state photodissociation.⁶ The main formation of HKrCl occurs upon consequent annealing at about 30 K, which shows a significant kinetic H/D isotope effect attributed to different thermal mobility of H and D atoms in solid krypton.⁷ HKrCl is one of the few noble-gas hydrides, for which all fundamental modes have been observed in the IR spectra.⁸

The complexes of noble-gas hydrides with other molecules have been studied both theoretically and experimentally.^{10–17} The HNgY complexes exhibit large blue shifts of the H–Ng stretching modes, which seems to be a normal effect for this type of molecule.¹¹ It is remarkable that the blue shifts of the H–Ng stretching modes are observed not only upon direct hydrogen bonding but also for van der Waals complexes without hydrogen bonding. The complex of HKrCl with nitrogen is among the experimentally observed systems.^{13,14}

Recently, we have studied the HXeY⋯HX (X, Y = HCl and HBr) complexes showing blue shifts of the H–Xe stretching mode up to +150 cm⁻¹ for the HXeBr⋯HBr complex.¹⁵ It is evidently interesting to expand this study to the HKrCl⋯HCl complex, which should intuitively undergo a very strong complexation effect due to weak intrinsic bonding of HKrCl.

Our experimental studies in a Kr matrix are supported by ab initio calculations at the MP2 level of theory.

2. Computational Details and Results

The computations were carried out by using the GAUSSIAN 03 program package on a Sun Fire 25K computer (CSC-IT Center for Science, Espoo, Finland).¹⁸ The second-order Møller–Plesset perturbation theory (MP2) was employed for the electron correlation together with the standard split-valence 6-311++G(2d,2p) (basis 1) and Dunning's aug-cc-pVTZ (basis 2) basis sets.¹⁹ In the following, the results obtained with basis 1 are mainly discussed. The calculations with basis 2 verify the data obtained with basis 1. The Bery optimization algorithm was used with the tight convergence criteria.¹⁸ Pulay's Direct Inversion in the Iterative Subspace extrapolation method was used for the self-consistent field procedure.²⁰

The charge distributions were obtained with the natural population analysis (NPA) method.²¹ The harmonic approximation was used for the vibrational potential energy surface calculations. The intermolecular interaction energies were calculated as a difference between the complex and the monomer energies taking into account the counterpoise basis set superposition error (BSSE) correction.²² Similar computational methods have been previously used for a number of HNgY complexes.¹¹

The calculations revealed three stable HKrCl⋯HCl complex structures (see Figure 1 and Table 1). The HCl molecule is attached to the Cl end of the HKrCl molecule in the two bent structures. The third complex (structure 3) is formed by interaction between the hydrogen atom of HKrCl and the HCl molecule, where the Cl atom of HCl is close to the HKrCl axis and HCl makes an angle of ~100° with this axis. The complexation leads to a substantial intramolecular reorganization (Table 1) accompanied with charge redistribution (Table 2). In structure 1, the two Cl atoms have substantially closer partial charges than in the monomers. In structures 2 and 3, the charge separation is smaller than in structure 1. For all three structures, the complexation increases the (HKr)⁺ partial charge, indicating

* To whom correspondence should be addressed. E-mail: leonid.khriachtchev@helsinki.fi.

† Current address: Jet Propulsion Laboratory, California Institute of Technology, 4800 Oak Grove Drive, Pasadena, CA 91109.

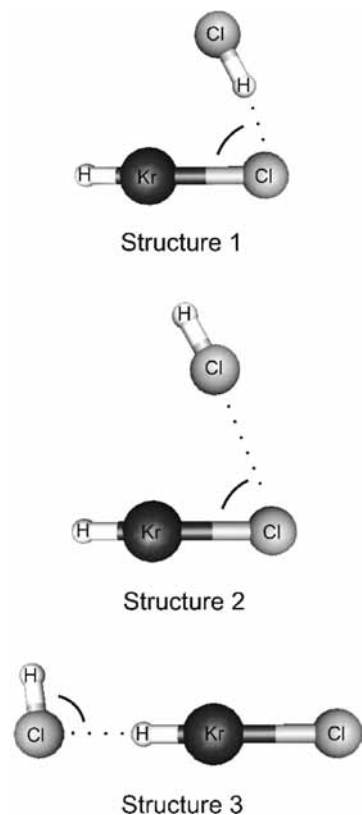


Figure 1. Computational minimum energy structures of the HKrCl...HCl complex. The structural parameters obtained at different levels of theory are given in Table 1.

TABLE 1: Computational Geometries of the Monomers and Complex Structures (See Figure 1)^a

	$r(\text{H}-\text{Kr})$	$r(\text{Kr}-\text{Cl})$	$r(\text{Cl}\cdots\text{H}/\text{Cl})$	$r(\text{H}-\text{Cl})$	angle
HKrCl and HCl monomers					
basis 1	1.500	2.551		1.270	
basis 2	1.484	2.500		1.271	
HKrCl...HCl complex					
structure 1, basis 1	1.465	2.620	2.050	1.315	78.0
structure 1, basis 2	1.453	2.573	2.016	1.315	76.2
structure 2, basis 1	1.496	2.556	3.600	1.271	70.6
structure 2, basis 2	1.480	2.507	3.439	1.273	70.2
structure 3, basis 1	1.490	2.608	2.248	1.274	98.1
structure 3, basis 2	1.473	2.559	2.221	1.275	97.3

^a The calculations are performed at the MP2 level of theory with the following basis sets: 6-311++G(2d,2p) (basis 1) and aug-cc-pVTZ (basis 2). The bond lengths are in Ångstroms, and the angles are in degrees.

the strengthening of the H–Kr covalent bond, which is accompanied with its shortening. No substantial differences in the complex geometries and partial charges are obtained for the two basis sets used, which suggests a small probability of computational artifacts.¹⁵

Structure 1 is the strongest complex with an interaction energy of ca. -3000 cm^{-1} (-36 kJ mol^{-1} , basis 1). The interaction in structures 2 and 3 is several times weaker (see Table 3). It is possible that the strong interaction in structure 1 is not only an effect of enhanced dipole–dipole arrangement but also due to the increased delocalized electron density, which provides a stabilizing effect from the ion-pair $(\text{HKr})^+\cdots(\text{ClHCl})^-$ structure. Structures 2 and 3 are characterized with a more usual dipole–dipole interaction. Structures 1 and 3 exhibit hydrogen bonding between the complex partners, whereas structure 2

TABLE 2: NPA Charges of the Monomers and Complex Structures (See Figure 1)^a

	HKrCl			HCl	
	$q(\text{H})$	$q(\text{Kr})$	$q(\text{Cl})$	$q(\text{H})$	$q(\text{Cl})$
HKrCl and HCl monomers					
basis 1	0.114	0.560	-0.674	0.250	-0.250
basis 2	0.112	0.564	-0.675	0.256	-0.256
HKrCl...HCl complex					
structure 1, basis 1	0.175	0.590	-0.670	0.263	-0.358
structure 1, basis 2	0.173	0.592	-0.662	0.264	-0.367
structure 2, basis 1	0.118	0.564	-0.678	-0.244	0.240
structure 2, basis 2	0.117	0.568	-0.679	-0.253	0.247
structure 3, basis 1	0.154	0.548	-0.761	-0.212	0.270
structure 3, basis 2	0.153	0.550	-0.761	-0.219	0.277

^a The calculations are performed at two levels of theory.

TABLE 3: Computational Interaction Energies for the Three HKrCl...HCl Structures (in cm^{-1})^a

	structure 1	structure 2	structure 3
$E(\text{int})$			
basis 1	-3463.2	-762.6	-1193.0
basis 2	-4033.7	-1101.9	-1793.9
$E(\text{int, BSSE})$			
basis 1	-3037.3	-442.3	-846.0
basis 2	-3440.3	-710.0	-1026.1

^a The energies are shown with and without BSSE correction obtained at two levels of theory.

TABLE 4: Computational Vibrational Frequencies of HKrCl and HCl Monomers and Shifts for the Three HKrCl...HCl Complexes (in cm^{-1}) Obtained at Two Levels of Theory^a

	monomer	structure 1	structure 2	structure 3
$\nu(\text{H}-\text{Kr})$				
basis 1	1828.8 (2411)	+251.5 (1121)	+24.3 (2211)	+81.8 (19)
basis 2	1947.2 (1941)	+222.8 (883)	+22.5 (1731)	+88.7 (4)
$\nu(\text{H}-\text{Cl})$				
basis 1	2998.1 (52)	-603.7 (1536)	-16.0 (32)	-37.5 (93)
basis 2	3057.6 (50)	-612.6 (1532)	-18.4 (27)	-37.5 (91)

^a The band intensities (in km mol^{-1}) are shown in parentheses.

forms a van der Waals complex without hydrogen bonding. In the previous work on the $\text{HXeY}\cdots\text{HX}$ complexes (X, Y = Br and Cl), the structural results were qualitatively similar to the present case.¹⁵ The BSSE correction substantially weakens the computed interaction, which is typical for noble-gas hydride complexes.¹¹

Table 4 presents the computed vibrational shifts of the H–Kr and H–Cl stretching modes for the studied complexes. It should be mentioned here that the H–Kr stretching frequency of HKrCl monomer is overestimated in the present calculations, which is a common situation for this computational method.^{1,3} All complex structures obtained in the present work have only real vibrational frequencies, which indicates true local minima on the potential energy surface. The vibrational spectra obtained with the two basis sets agree with each other quite well. For structure 1, the complexation-induced blue shift of the H–Kr stretching mode is very large ($+251\text{ cm}^{-1}$ with basis 1). Structure 2 and structure 3 exhibit substantially smaller shifts of ca. $+20$ and $+80\text{ cm}^{-1}$, respectively. The $\nu(\text{H}-\text{Kr})$ blue shifts originate from the charge redistribution in the HKrCl molecule upon complexation, which enhances its $(\text{HKr})^+\text{Cl}^-$ ion-pair character. This charge redistribution correlates with the shorten-

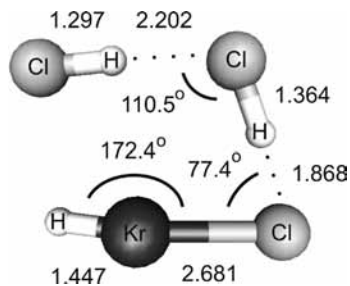


Figure 2. Computational structure of the HKrCl...HCl complex (mixed trimer). The bond lengths are in Ångstroms.

ing of the H–Kr bond, blue shift of the H–Kr stretching frequency, and decrease of the absorption intensity.

The HCl absorption intensity is strongly enhanced upon complexation from 50 km mol⁻¹ calculated for the monomer to ca. 1500 km mol⁻¹ in structure 1. The enhancement of absorption intensity is accompanied with a strong $\nu(\text{H–Cl})$ red shift of ca. -600 cm^{-1} from the monomeric value. The HCl absorption intensity is somewhat increased in structure 3 ($\sim 100\text{ km mol}^{-1}$), and the frequency red shift is also moderate (37.5 cm^{-1}).

For the previously studied HXeCl...HCl complex, the H–Xe stretching shifts are smaller ($+126$, $+9$, and $+49\text{ cm}^{-1}$ with basis 1 for structures 1, 2, and 3, respectively).¹⁵ The strongest HXeCl...HCl complex (structure 1) has a computed interaction energy of -2754 cm^{-1} . Thus, the complexation effect is stronger for HKrCl...HCl than for HXeCl...HCl, which can be connected with weaker intrinsic bonding of HKrCl as compared to HXeCl.

In addition to the HKrCl...HCl complex, we studied the HKrCl...HCl complex (mixed trimer) using basis 1 and considering only a geometry shown in Figure 2. This geometry is a combination of the strongest HKrCl...HCl complex (structure 1) and the strongest HCl dimer. The computational monomer-to-complex shifts are $+420\text{ cm}^{-1}$ for the H–Kr stretching vibration and -1200 cm^{-1} for one of the HCl molecules. The H–Kr partial charge increases in the mixed trimer to a value of $+0.82$, which explains the large blue shift of the H–Kr stretching mode as compared with the monomer. The interaction energy of the HKrCl...HCl complex without BSSE correction is -6236 cm^{-1} (-75 kJ mol^{-1}). For the HXeBr...HBr complex, the computational H–Xe stretching shift is $+252\text{ cm}^{-1}$,¹⁵ that is, substantially smaller than in the present case.

3. Experimental Details and Results

The HCl/Kr mixtures with concentrations from 1/100 to 1/2000 were deposited onto a cold CsI substrate at temperatures from 20 to 35 K in a closed-cycle helium cryostat (APD, DE 202A). The IR absorption spectra in the 4000 to 400 cm^{-1} range were measured with a Nicolet SX60 FTIR spectrometer (resolution 1 cm^{-1}). The matrices were photolyzed with a 193 nm excimer laser (MPB, MSX-250, pulse energy density $\sim 10\text{ mJ cm}^{-2}$). The photolyzed matrices were annealed at 30–45 K, and the IR spectra were measured at 8.5 K.

Deposition of diluted HCl/Kr mixtures (1/1000 to 1/2000) at relatively low temperatures (20–30 K) leads to predominantly monomeric HCl in solid krypton. The assignment of the monomeric bands was done long ago in terms of HCl rotation, and the main R(0) component is observed at 2873 cm^{-1} .^{23,24} The bands of HCl multimers appear in the IR spectrum when the deposition temperature and HCl concentration increase (see

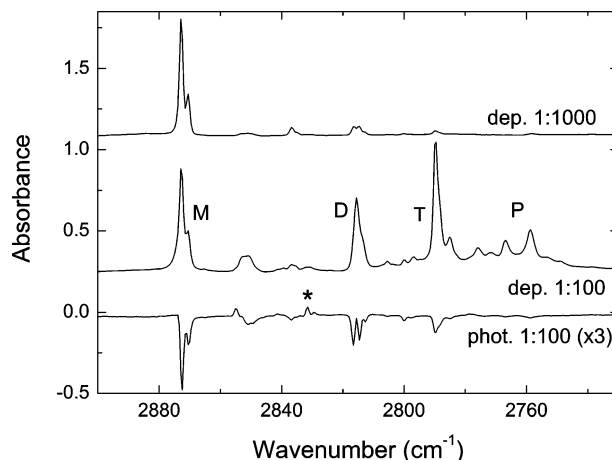


Figure 3. IR spectra of two HCl/Kr (1/1000 and 1/100) matrices deposited at 35 K and a difference spectrum showing the result of 193 nm photolysis (600 pulses) of the more concentrated matrix. The bands of HCl monomers (M), dimers (D), trimers (T), and higher polymers (P) are marked.^{23,24} The band at 2831.5 cm^{-1} marked with an asterisk presumably belongs to the Cl...HCl complex.^{26,27} The spectra were measured at 8.5 K.

Figure 3). The HCl bands decrease upon 193 nm photolysis, reflecting the HCl photodissociation. The HCl decomposition in thick and concentrated matrices is complicated by self-limitation of photolysis.²⁵ A number of new bands appear upon photolysis. The rising 2831.5 cm^{-1} band marked in Figure 3 by asterisk presumably belongs to the Cl...HCl complex.^{26,27} The $(\text{KrHKr})^+$ bands (strongest at 852.4 cm^{-1}) are also seen after photolysis (ref 28) as well as the HKrCl bands showing the locality of photolysis as discussed elsewhere.⁶

Annealing at about 30 K mobilizes H atoms in solid krypton, and HKrCl molecules are formed in the H + Kr + Cl reaction of the neutral atoms (see Figure 4a).⁷ For matrices with small HCl/Kr ratios (1/1000 to 1/2000), the HKrCl monomer strongly dominates in the spectrum. For higher HCl concentrations, additional peaks are observed through the broad spectral region after annealing (see Figure 4b), and the strongest of them are listed in Table 5. No corresponding bands appear in similar experiments in Ar matrices; that is, they are specific to a Kr matrix. The 2831.5 cm^{-1} band of the HCl...Cl complex substantially decreases upon annealing. Some of the bands seen in Figure 4 (for example, at 1830 and 2320 cm^{-1}) are not well reproducible, whereas the other bands appear in all experiments. No satellites of the HKrCl bending mode (544 cm^{-1}) are observed at higher HCl concentrations, which is presumably due to the low signal-to-noise ratio in this spectral region.

The IR spectrum depends on the annealing temperature as seen in Figure 5. In particular, the band at 1546 cm^{-1} increases upon annealing at higher temperatures, whereas the 1589 cm^{-1} band decreases. Annealing at 45 K strongly enhances a band at 2155 cm^{-1} and its broader satellite at $\sim 2200\text{ cm}^{-1}$. The concentration-enhanced bands can be easily decomposed by 193 nm light quite synchronously with the HKrCl monomer as demonstrated in Figure 6. The 193 nm irradiation substantially recovers the 2831.5 cm^{-1} band of the HCl...Cl complex.

4. Discussion and Conclusions

The new bands observed for photolyzed and annealed matrices with high HCl/Kr ratios are assigned to complexes between HKrCl and HCl (see Table 5). Higher deposition temperatures and larger HCl concentrations lead to HCl multimers (see Figure 3), which principally allows the HKrCl...HCl

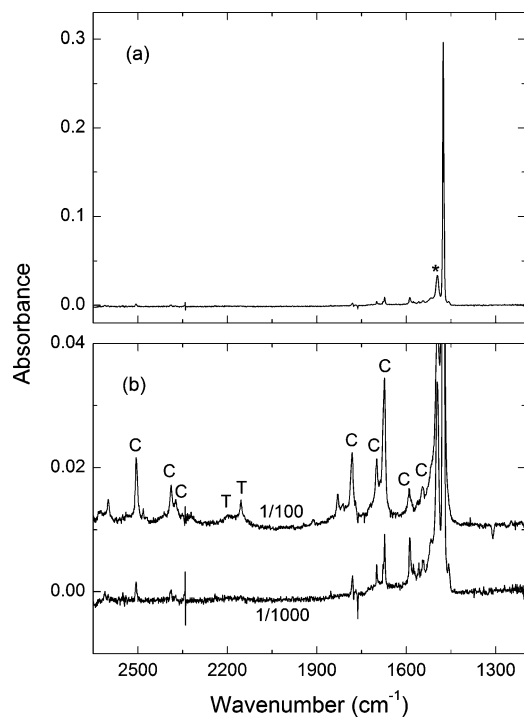


Figure 4. (a) IR difference spectrum showing the result of annealing at 30 K (5 min) for the photolyzed HCl/Kr (1/1000) matrix. The band marked with an asterisk originates from librational motion of HKrCl in solid krypton.⁹ (b) Vertically expanded spectra showing the results of annealing at 30 K for two HCl/Kr (1/100 and 1/1000) matrices. The matrices were deposited at 35 K and photolyzed at 193 nm. The spectra were measured at 8.5 K. The bands assigned to the HKrCl...HCl (C) and HKrCl...HCl₂ (T) are marked. The band assignment is given in Table 5.

TABLE 5: Experimental Frequencies (in cm⁻¹) of Annealing-Induced Bands with the Most Probable Assignments^a

frequency	molecule	shift	structure
1476	HKrCl	0	monomer
1496	HKrCl	+20	libration ^b
1546	HKrCl	+70	structure 3
1589	HKrCl	+113	structure 3
1673	HKrCl	+197	structure 1
1699	HKrCl	+223	structure 1
1782	HKrCl	+306	structure 1
2155	HCl	-718	trimer ^c
2200	HKrCl	+724	trimer ^c
2373	HCl	-500	structure 1
2388	HCl	-485	structure 1
2506	HCl	-367	structure 1

^aThe shifts (in cm⁻¹) are calculated with respect to the corresponding monomers (the HCl monomer absorbs at 2873 cm⁻¹). The complex structures are presented in Figures 1 and 2. ^b See ref 9. ^c Tentative assignment.

formation. The HKrCl molecules can be easily decomposed by UV light.⁶ The efficient decomposition of the new bands synchronously with the HKrCl monomers confirms that HKrCl participates in the corresponding species. The blue shift of the H–Kr stretching mode is a normal effect for HNgY complexes.¹¹

The structural assignment is based on the computational vibrational properties. Two absorption bands, shifted by +70 and +113 cm⁻¹ from the monomeric band, are assigned to structure 3, which has a theoretical shift of +82 cm⁻¹ (basis 1). The higher-energy band appears at lower annealing tem-

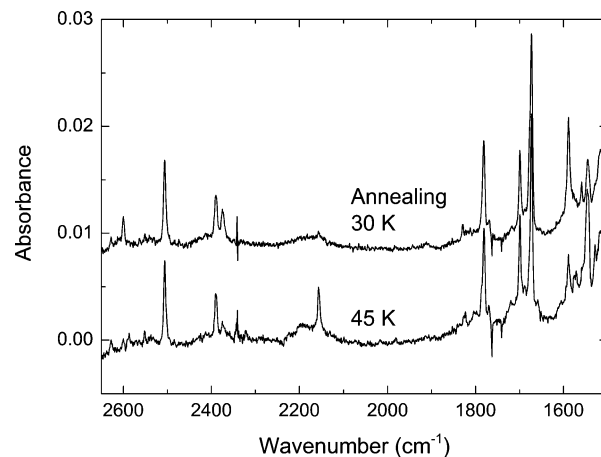


Figure 5. IR difference spectra showing the results of annealing at different temperatures 30 and 45 K (5 min) for the HCl/Kr (1/250) matrix deposited at 35 K and photolyzed with 193 nm light. The spectra were measured at 8.5 K. The band assignment is given in Table 5.

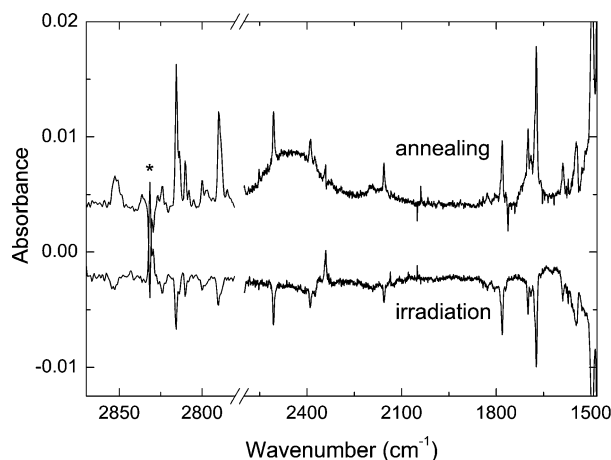


Figure 6. IR difference spectra showing the results of annealing at 40 K (5 min) and consequent irradiation (193 nm, 80 pulses). The band at 2831.5 cm⁻¹ marked with an asterisk presumably belongs to the Cl...HCl complex.^{26,27} The data are obtained for an HCl/Kr (1/250) matrix deposited at 35 K and photolyzed with 193 nm light. Notice the change of scale after axis break. The spectra were measured at 8.5 K. The band assignment is given in Table 5.

peratures, and it decreases at higher temperatures (45 K), whereas the lower-energy band increases. This spectral change may indicate conversion of the corresponding structures in the matrix, similarly to well-known matrix-site thermal conversion.^{29,30} We speculate that these two bands correspond to structure 3 differently perturbed by the matrix, and thermal annealing converts the system to a lower-energy configuration. No HCl bands corresponding to structure 3 were found, which is explained by their relatively low intensity and probable overlap with the HCl multimeric bands. It should be mentioned that the H–Kr stretching band with the +113 cm⁻¹ shift appears practically at the same position as the HKrCl...N₂ complex (linear structure); however, we have no additional indications for this nitrogen complex. The HCl...N₂ complex is not seen after deposition in sufficient amounts, and the main band of the HKrCl...N₂ complex (bent structure) with the +32.4 cm⁻¹ shift is not observed after annealing.^{13,14} Furthermore, it seems improbable that the HKrCl...N₂ complex would decrease upon higher-temperature annealing (see Figure 5).

The formation path of the HKrCl...HCl complex with structure 3 is somewhat uncertain because it requires two

precursor HCl molecules in the neighboring cages (see Figure 1). First, it should be noted that structure 3 cannot be enhanced by preparation of more HCl dimers because the heavier Cl atoms should appear in different matrix cages. It follows that the amount of this complex after annealing should not straightforwardly correlate with the HCl concentration when the amount of the HCl dimers increases. This was actually observed in the experiment because the two bands assigned to structure 3 are observed at lower HCl concentrations as compared to the other complex bands. Second, the bands assigned to structure 3 are enhanced upon longer photolysis. This experimental fact can be readily interpreted in terms of light-induced mobility of Cl atoms due to charge-transfer excitation in a Kr matrix.³¹ The recombination of charges can in principle move matrix-isolated species due to structural relaxation involving matrix atoms.

Three bands shifted by +197, +223, and +306 cm^{-1} from the HKrCl monomer are assigned to the H–Kr stretching mode in structure 1 of the HKrCl···HCl complex in different matrix configurations. Structure 1 has a computational shift of +252 cm^{-1} (basis 1), which is similar to the experimental values. In the numerous experiments with different HCl concentrations and deposition temperatures, the relative intensity of these three bands remains quite similar. This suggests that all of these bands most probably originate from the 1:1 complexes with the same approximate structure differently perturbed by the local matrix morphology. A similar band splitting has been observed for other noble-gas hydride complexes; in particular, four H–Xe stretching bands of the HXeCl···HCl complex in a Xe matrix were assigned to structure 1.¹⁵ The previously studied HXeCl···HCl complex (structure 1) exhibits experimental blue shifts up to 116 cm^{-1} , which are quite smaller than in the present case of HKrCl···HCl, in agreement with the theory.

Decomposition of the HKrCl···HCl complex by light increases the 2831.5 cm^{-1} band of the HCl···Cl complex featuring its release from the HKrCl···HCl complex (see Figure 6). The intensity of the three H–Kr stretching bands assigned to structure 1 correlates with the amount of HCl dimers after deposition and with the 2831.5 cm^{-1} band of the HCl···Cl complex seen after photolysis. It is clear from Figure 1 that structure 1 can originate from reactions of mobile H atoms with the Kr···Cl···HCl centers.

Three bands are found at 2373, 2388, and 2506 cm^{-1} , which can be assigned to the HCl absorption in structure 1 (see Table 5). This is a reasonable suggestion due to the high absorption intensity of complexed HCl, which is computationally ca. 1500 km mol^{-1} . The computational red shift of ca. –600 cm^{-1} agrees with the experimental values from –360 to –500 cm^{-1} . These three HCl bands rise and bleach synchronously with the HKrCl bands of structure 1, which supports the present assignment. However, we cannot establish an explicit correspondence between the individual HCl and HKrCl bands in the complex. The computational data suggest that an increased blue shift of the H–Kr stretching bands should correlate with an increased red shift of the HCl bands. The observation of the HCl absorptions of the HKrCl···HCl complex is a remarkable difference from the previous studies of the HNgY complexes where the H–Ng stretching bands were exclusively observed.

Structure 2 of the HKrCl···HCl complex has not been found in these experiments, which is probably due to the weak interaction (see Table 3). The species in structure 2 might be converted to structure 1 upon annealing if the conversion barrier is low enough.

Two additional bands at 2155 and 2200 (broad) cm^{-1} are formed upon annealing. We tentatively assign these bands to

the HKrCl···(HCl)₂ complex (mixed trimer). These bands appear only for the higher HCl/Kr concentrations (1/100 to 1/250) where the Cl···(HCl)₂ intermediate can be formed (although not identified in experiment), and they are enhanced upon higher-temperature annealing (40–45 K). The latter fact can be adequately explained by thermal mobility of residual HCl in solid krypton. In our recent study on the HXeCCH···HCCH complexes, the complex formation has been entirely explained by thermal mobilization of acetylene in solid xenon.¹⁷ We tentatively suggest that the sharper band at 2155 cm^{-1} is the HCl absorption and the broadband at 2200 cm^{-1} originates from the H–Kr stretching mode. The H–Ng stretching modes often show broad absorptions due to extensive environmental effects. The computations predict the highest intensity in this complex for the HCl absorption (>3000 km mol^{-1}), which points to the 2155 cm^{-1} band. The experimental shifts for the HCl and H–Kr stretching absorptions are –718 and +724 cm^{-1} , which is in a good balance with computationally predicted –1200 and +420 cm^{-1} . It is seen that the computations predict smaller H–Kr stretching shift as compared to the experimental candidate. This numerical discrepancy can be caused by the overestimated computational stability of HKrCl. In turn, the too high computational red shift of HCl may be connected with an overestimated interaction in the complex. The higher HKrCl···(HCl)_n ($n \geq 3$) complexes may contribute to the spectrum after annealing. The chance to obtain (HKrCl)_n ($n \geq 2$) structures remains an open question.

Thus, the present results feature the HKrCl complexes with HCl in a Kr matrix. The HKrCl···HCl complex exhibits a blue shift of the H–Kr stretching mode in comparison with the HKrCl monomer, which is caused by enhanced (HKr)⁺Cl[–] charge separation and indicates stabilization of the H–Kr bond upon complexation. The obtained maximal shift of ca. +300 cm^{-1} is probably the largest blue shift experimentally observed for 1:1 molecular complexes. The corresponding HCl absorptions are also found with red shifts as large as ca. –500 cm^{-1} . The HKrCl···(HCl)₂ mixed trimer is tentatively identified, and it shows a huge blue shift of the H–Kr stretching mode (ca. +700 cm^{-1}). The ab initio calculations at the MP2 level of theory fully support these conclusions.

Acknowledgment. The work was supported by the Finnish Center of Excellence in Computational Molecular Science. A.C. is a member of the International Master's Degree Programme in Advanced Spectroscopy in Chemistry (ASC). A.D. acknowledges a postdoctoral grant from the University of Helsinki. A.L. acknowledges a research grant from the Academy of Finland. CSC–IT Center for Science Ltd. is thanked for computational resources.

References and Notes

- (1) Khriachtchev, L.; Räsänen, M.; Gerber, R. B. *Acc. Chem. Res.* **2009**, *42*, 183.
- (2) Grochala, W. *Chem. Soc. Rev.* **2007**, *36*, 1632.
- (3) Lundell, J.; Khriachtchev, L.; Pettersson, M.; Räsänen, M. *Low Temp. Phys.* **2000**, *26*, 680.
- (4) Khriachtchev, L.; Pettersson, M.; Runeberg, N.; Lundell, J.; Räsänen, M. *Nature (London)* **2000**, *406*, 874.
- (5) Pettersson, M.; Lundell, J.; Räsänen, M. *J. Chem. Phys.* **1995**, *102*, 6423.
- (6) Khriachtchev, L.; Pettersson, M.; Lundell, J.; Räsänen, M. *J. Chem. Phys.* **2001**, *114*, 7727.
- (7) Khriachtchev, L.; Saarelainen, M.; Pettersson, M.; Räsänen, M. *J. Chem. Phys.* **2003**, *118*, 6403.
- (8) Lignell, A.; Lundell, J.; Pettersson, M.; Khriachtchev, L.; Räsänen, M. *Low Temp. Phys.* **2003**, *29*, 844.
- (9) Khriachtchev, L.; Lignell, A.; Juselius, J.; Räsänen, M.; Savchenko, E. *J. Chem. Phys.* **2005**, *122*, 014510.

- (10) McDowell, S. A. C. *Curr. Org. Chem.* **2006**, *10*, 791.
- (11) Lignell, A.; Khriachtchev, L. *J. Mol. Struct.* **2008**, *889*, 1.
- (12) Nemukhin, A. V.; Grigorenko, B. L.; Khriachtchev, L.; Tanskanen, H.; Pettersson, M.; Räsänen, M. *J. Am. Chem. Soc.* **2002**, *124*, 10706.
- (13) Lignell, A.; Khriachtchev, L.; Pettersson, M.; Räsänen, M. *J. Chem. Phys.* **2002**, *117*, 961.
- (14) Lignell, A.; Khriachtchev, L.; Pettersson, M.; Räsänen, M. *J. Chem. Phys.* **2003**, *118*, 11120.
- (15) Lignell, A.; Lundell, J.; Khriachtchev, L.; Räsänen, M. *J. Phys. Chem. A* **2008**, *112*, 5486.
- (16) Tanskanen, H.; Johansson, S.; Lignell, A.; Khriachtchev, L.; Räsänen, M. *J. Chem. Phys.* **2007**, *127*, 154313.
- (17) The HXeCCH complex with acetylene has been recently studied by Domanskaya, A.; Kobzareno, A. V.; Tsivion, E.; Khriachtchev, L.; Feldman, V. I.; Gerber, R. B.; Räsänen, M. The HXeCCH molecules were formed at 40 K upon mobility of H atoms in solid xenon, whereas the HXeCCH \cdots HCCH complex was formed at ca. 55 K together with acetylene agglomerates.
- (18) Frisch, M. J.; Trucks, G. W.; Schlegel, H. B.; Scuseria, G. E.; Robb, M. A.; Cheeseman, J. R.; Montgomery, J. A., Jr.; Vreven, T.; Kudin, K. N.; Burant, J. C.; Millam, J. M.; Iyengar, S. S.; Tomasi, J.; Barone, V.; Mennucci, B.; Cossi, M.; Scalmani, G.; Rega, N.; Petersson, G. A.; Nakatsuji, H.; Hada, M.; Ehara, M.; Toyota, K.; Fukuda, R.; Hasegawa, J.; Ishida, M.; Nakajima, T.; Honda, Y.; Kitao, O.; Nakai, H.; Klene, M.; Li, X.; Knox, J. E.; Hratchian, H. P.; Cross, J. B.; Bakken, V.; Adamo, C.; Jaramillo, J.; Gomperts, R.; Stratmann, R. E.; Yazyev, O.; Austin, A. J.; Cammi, R.; Pomelli, C.; Ochterski, J. W.; Ayala, P. Y.; Morokuma, K.; Voth, G. A.; Salvador, P.; Dannenberg, J. J.; Zakrzewski, V. G.; Dapprich, S.; Daniels, A. D.; Strain, M. C.; Farkas, O.; Malick, D. K.; Rabuck, A. D.; Raghavachari, K.; Foresman, J. B.; Ortiz, J. V.; Cui, Q.; Baboul, A. G.; Clifford, S.; Cioslowski, J.; Stefanov, B. B.; Liu, G.; Liashenko, A.; Piskorz, P.; Komaromi, I.; Martin, R. L.; Fox, D. J.; Keith, T.; Al-Laham, M. A.; Peng, C. Y.; Nanayakkara, A.; Challacombe, M.; Gill, P. M. W.; Johnson, B.; Chen, W.; Wong, M. W.; Gonzalez, C.; Pople, J. A. *Gaussian 03*, revision C.02; Gaussian, Inc.: Wallingford, CT, 2004.
- (19) Schuchardt, K. L.; Didier, B. T.; Elsethagen, T.; Sun, L.; Gurmooorthi, V.; Chase, J.; Li, J.; Windus, T. L. *J. Chem. Inf. Model.* **2007**, *47*, 1045.
- (20) Pulay, P. *J. Comput. Chem.* **1982**, *3*, 556.
- (21) Reed, A. E.; Curtiss, L. A.; Weinhold, F. *Chem. Rev.* **1988**, *88*, 899.
- (22) Boys, S. F.; Bernardi, F. *Mol. Phys.* **1970**, *19*, 553.
- (23) Mann, D. E.; Acquista, N.; White, D. *J. Chem. Phys.* **1966**, *44*, 3453.
- (24) Bowers, M. T.; Flygare, W. H. *J. Chem. Phys.* **1966**, *44*, 1389.
- (25) Khriachtchev, L.; Pettersson, M.; Räsänen, M. *Chem. Phys. Lett.* **1998**, *288*, 727.
- (26) Lorenz, M.; Kraus, D.; Räsänen, M.; Bondybey, V. E. *J. Chem. Phys.* **2000**, *112*, 3803.
- (27) Dickgiesser, M.; Schwentner, N. *Nucl. Instrum. Methods B* **2000**, *168*, 252.
- (28) Bondybey, V. E.; Pimentel, G. C. *J. Chem. Phys.* **1972**, *56*, 3832.
- (29) Khriachtchev, L.; Pettersson, M.; Lignell, A.; Räsänen, M. *J. Am. Chem. Soc.* **2001**, *123*, 8610.
- (30) Bochenkova, A. V.; Bochenkov, V. E.; Khriachtchev, L. *J. Phys. Chem. A* **2009**, *113*, 7654.
- (31) Fajardo, M. E.; Withnal, R.; Feld, J.; Okada, F.; Lawrence, W.; Wiedeman, L.; Apkarian, V. A. *Laser Chem.* **1988**, *9*, 1.

JP9044622